

# Limits on Topological Defects Models of the Ultrahigh Energy Cosmic Rays \*

R.J. Protheroe<sup>1</sup> and Todor Stanev<sup>2</sup>

<sup>1</sup>*Department of Physics and Mathematical Physics, University of Adelaide  
Adelaide, SA 5000, Australia*

<sup>2</sup>*Bartol Research Institute, University of Delaware, Newark, DE 19716, U.S.A.*

Using the propagation of ultra high energy nucleons, photons and electrons in the universal radiation backgrounds, we obtain limits on the luminosity of topological defects scenarios for the origin of the highest energy cosmic rays. The limits are set as function of the mass of the X-particles emitted by the cosmic strings or other defects, the cosmological evolution of the topological defects, and the strength of the extragalactic magnetic fields. The existing data on the cosmic ray spectrum and on the isotropic 100 MeV gamma-ray background limit significantly the parameter space in which topological defects can generate the flux of the highest energy cosmic rays.

PACS numbers: 98.35.Eg, 98.70.Sa, 98.70.Vc, 98.80.Cq

The cosmic ray events with the highest energies so far detected have energies of  $2 \times 10^{11}$  GeV [1] and  $3 \times 10^{11}$  GeV [2]. The question of the origin of these cosmic rays having energy significantly above  $10^{11}$  GeV is complicated by propagation of such energetic particles through the universe. The threshold for pion photoproduction on the microwave background is  $\sim 2 \times 10^{10}$  GeV, and at  $3 \times 10^{11}$  GeV the energy-loss distance is about 20 Mpc. Propagation of cosmic rays over substantially larger distances gives rise to a cut-off in the spectrum at  $\sim 10^{11}$  GeV as was first shown by Greisen [3], and Zatsepin and Kuz'min [4], the “GZK cut-off”.

The standard cosmic ray acceleration mechanism, shock acceleration, leads to a power-law energy spectrum,  $dn/dE \propto E^{-\alpha}$ , with differential index  $\alpha > 2$ , extending up to a maximum energy which is determined by the physical conditions at the acceleration site, the most important being its physical dimensions and magnetic field. To reach energies of  $\sim 10^{11}$  GeV one requires the conditions present in powerful radio galaxies [5]. However, there seem to be no suitable powerful radio galaxies sufficiently close to explain the  $2-3 \times 10^{11}$  GeV events.

One exciting possible explanation of the highest energy cosmic rays is the topological defect (TD) scenario [6-9], where the observed cosmic rays are a result of top-down cascading, from somewhat below (depending on theory) the GUT scale energy of  $\sim 10^{16}$  GeV, down to  $10^{11}$  GeV and lower energies. Generally, these models put out much of the energy in a very flat spectrum of photons and electrons extending up to the mass of the “X-particles” emitted. Approximating this spectrum by monoenergetic injection of photons of energy  $10^{15}$  GeV, Protheroe and Johnson [10] showed that spectra from single TD sources

can not explain the  $2-3 \times 10^{11}$  GeV events. However, some support for a new high energy component comes from the possible presence of a gap in the spectrum between  $10^{11}$  GeV and  $2 \times 10^{11}$  GeV [11], although more data are required to confirm this.

The main problem with topological defect models is the wide range of model parameters in which this scenario could, in principle, be applied. Parameters of TD scenarios include: mass of the X-particle, energy spectra and final state composition of the decay products, and cosmological evolution of the topological defect injection rate [12,13]. The problem of propagation is more severe than for the case of acceleration scenarios because most of the energy from X-particle decay emerges in electrons, photons and neutrinos, with only about 3% in nucleons. The electrons and photons initiate electromagnetic cascades in the extragalactic radiation fields and magnetic field, resulting in a complicated spectrum of electrons and photons which is very sensitive to the radiation and magnetic environment. For example, recently the HEGRA group [14] have placed an upper limit on the ratio of  $\gamma$ -rays to cosmic rays of  $\sim 10^{-2}$  at  $10^5$  GeV and, using a TD model calculation [7] which neglected the IR background and gave a higher ratio, argued that TD models were ruled out. However, inclusion of the IR would reduce the  $10^5$  GeV  $\gamma$ -ray intensity to well below the HEGRA limit.

Protheroe and Johnson [15] considered one set of parameters ( $M_X c^2 = 10^{15}$  GeV, constant injection per co-moving volume,  $B = 10^{-9}$  gauss) and ruled out TD as the origin of the  $2-3 \times 10^{11}$  GeV events. More recently, Lee [13] and Sigl, Lee and Coppi [16], adopting  $M_X c^2 = 10^{14}$  GeV, and a lower magnetic field, claimed the TD scenario is not ruled out. In this letter we consider several TD scenarios to put limits on the luminosity of the particle fluxes injected by topological defects as a function of the X-particle mass, the cosmological evolution of the topological defects and the strength of the extragalactic magnetic field, and consider for what range of parameters TD could explain the  $2-3 \times 10^{11}$  GeV events.

We use the same injection spectra and TD evolution as in ref. [16]. This is approximately an  $E^{-1.5}$  spectrum extending up to  $\sim M_X c^2/2$  containing  $\sim 3\%$  nucleons and  $97\%$  pions. In the matter dominated era of the universe, and assuming  $q_0 = 0.5$ , the injection rate per co-moving volume is  $Q(t) = Q_0(t/t_0)^{-2+p}$  where  $p = 1$  for ordinary cosmic strings and monopole-antimonopole annihilation,  $p = 0$  for superconducting cosmic strings, and  $p = 2$  for models with constant injection.

We inject this spectrum at various distances and carry out a Monte-Carlo matrix propagation calculation as described in ref. [10]. The following processes are included:  $\gamma\gamma \rightarrow e^+e^-$  on the microwave, radio and IR/optical background, IC scattering on the same backgrounds, triplet

production in the same environment, and neutron production and decay are taken into account.

For the radio background we use the spectrum of Clark et al. [17] which has been used previously in propagation calculations. This spectrum, which is based on interpretation of direct observations, has a low-frequency cut-off at  $\sim 1$  MHz. Other estimates of the radio background based on data on radio galaxies and ordinary galaxies give a radio background extending to significantly lower frequencies [18,19], and we shall discuss the effect of using different radio spectra elsewhere [20]. Magnetic field values we use are  $10^{-15}, 10^{-12}, 10^{-11}, \dots 10^{-8}$  G. The values at the high end of this range may be appropriate if topological defects are seeds for the formation of galaxies and larger structures in the universe [21] where fields are generally higher than average. For the infrared background we adopt a spectrum [22] which is based on the model of Stecker et al. [23] but constrained at low frequencies by upper limits derived by us from the error bars on the microwave background measured by the FIRAS experiment on COBE [24]. At  $3 \times 10^{-3}$  eV, where the microwave background is decreasing rapidly with energy, our IR spectrum is a factor of 5 lower than that used by Lee [13].

For a uniform distribution of topological defects we obtain the total intensity by integrating over redshift the results obtained for propagation over fixed distances, taking account of topological defect evolution and cosmological expansion assuming  $H_0 = 75$  km s $^{-1}$  Mpc $^{-1}$  and  $q_0 = 0.5$ . The result for  $M_X c^2 = 10^{14.1}$  GeV, a magnetic field of  $10^{-9}$  gauss, and  $p = 2$ , is shown in Fig. 1 where we have normalized the spectrum of “observable particles” (nucleons, photons, electrons) to the  $3 \times 10^{11}$  GeV point (cosmic ray data are taken from [25], and the highest point is from [2]). Lee [13] has published a spectrum for similar input parameters and it is in acceptable agreement with the present work except for MeV–PeV  $\gamma$ -rays where our result is about a factor of 10 lower. We suspect this is because of our lower IR field, and this appears to be confirmed by results presented by Lee which show the  $\gamma$ -ray intensity to be significantly lower if the IR field is neglected. With our lower IR field, and consequent lower  $\gamma$ -ray intensity, we are less likely to rule out topological defect models due to excess  $\gamma$ -ray production. For normalization to the  $3 \times 10^{11}$  GeV data, the injection rate of energy in X-particles would be  $\sim 6 \times 10^{-44}$  erg cm $^{-1}$  s $^{-1}$ . Notice that above  $10^{11}$  GeV photons dominate the spectra of observable particles, and that over some ranges of energy electrons dominate the electromagnetic component. Also note that the predicted  $\gamma$ -ray flux at GeV energies is comparable to the observed background, and as pointed out by Lee [13], the extragalactic  $\gamma$ -ray background at these energies will place a strong constraint on

Synchrotron radiation is very important in determining the  $\gamma$ -ray spectrum at MeV–PeV energies which can vary by orders of magnitude depending on the magnetic field. Limits on the injection rate obtained from comparing the predicted 0.1–10 GeV intensities with SAS-II [26] and preliminary EGRET [27] data are only lower than the injection rate obtained from normalization at  $3 \times 10^{11}$  GeV (and thus rule out a TD origin for the  $2\text{--}3 \times 10^{11}$  GeV events) for the highest magnetic fields. Where this limit is lower than the injection rate obtained from normalizing the intensity of observable particles to the  $3 \times 10^{11}$  GeV point, these limits have been added to Figure 2 for the three evolution models. We see that the  $\gamma$ -ray data provide the strongest constraint for models with high  $M_X$ , high  $B$  and weak evolution. No models with  $M_X c^2 < 10^{14.4}$  GeV are excluded by the constraints imposed so far, so if we used only these two constraints we would agree with Sigl et al. [16] that TD scenarios are not ruled out.

A further constraint, not considered by Sigl et al. [16], comes from the intensity of potentially observable particles above  $3 \times 10^{11}$  GeV. This constraint has already been used by Protheroe and Johnson [15] to rule out the model with  $M_X = 10^{15}$  GeV,  $p = 2$ , and  $B = 10^{-9}$  gauss. Here we use the fact that 1 event was observed by the Fly’s Eye between  $10^{11.45}$  GeV and  $10^{11.55}$  GeV, together with the published intensity at  $10^{11.5}$  GeV, to obtain the exposure factor of the Fly’s Eye experiment at this energy. Assuming the exposure factor has the same value also at higher energies (a reasonable assumption as at these energies optical transmission will limit the distance to observable air showers rather than the inverse-square law), we can estimate the number of events which should have been observed above  $3 \times 10^{11}$  GeV. Given that no events have been seen above this energy, we set a 90% upper limit of 2.3 events which, when compared with the expected number of events, sets a new upper limit to the rate of injection of energy in X-particles. This limit is approximately independent of topological defect evolution and is plotted in Figure 3 against  $M_X$  for various magnetic fields. In *all cases* this limit is lower than the injection rate required to explain the  $2\text{--}3 \times 10^{11}$  GeV events, and so it would appear that, subject to  $\gamma$ -rays and electrons above this energy being detectable by the Fly’s Eye as discussed below, topological defect models are ruled out as the explanation of the  $2\text{--}3 \times 10^{11}$  GeV events.

The limits on the injection rate of energy in X-particles from the number of “observable particles” above  $3 \times 10^{11}$  GeV may actually be weaker than given in Figure 3 because these particles are dominated by photons and electrons which might be undetectable. Energetic  $\gamma$ -rays entering the atmosphere will be subject to the LPM effect [28] (the suppression of electromagnetic cross-sections at

$5 \times 10^{11}$  GeV,  $8 \times 10^{11}$  GeV, and  $1.3 \times 10^{12}$  GeV for gamma-rays entering the atmosphere at  $\cos \theta = 1, 0.75$ , and  $0.5$  respectively. Such showers would be very difficult to reconstruct by experiments such as Fly's Eye and at best would be assigned a lower energy. In this case, we should treat electrons and  $\gamma$ -rays as unobservable, and normalize the *nucleon intensity* to the  $3 \times 10^{11}$  GeV data. This has the effect of increasing the predicted  $\gamma$ -ray intensities, and the new upper limits to the rate of injection of energy in X-particles would be as given in Figure 4. We now see that normalizing to the  $3 \times 10^{11}$  GeV data violates the  $\gamma$ -ray data for all models with  $p = 2$ , models with  $p = 1$  and  $M_X > 10^{13.1} - 10^{13.7}$  GeV depending on  $B$ , and models with  $p = 0$  and  $M_X > 10^{13.9} - 10^{14.9}$  GeV depending on  $B$ .

Before entering the Earth's atmosphere  $\gamma$ -rays and electrons are likely to interact on the geomagnetic field (see Erber [30] for a review of the theoretical and experimental understanding of the interactions). In such a case the  $\gamma$ -rays propagating perpendicular to the geomagnetic field lines would cascade in the geomagnetic field, i.e. pair production followed by synchrotron radiation. The cascade process would degrade the  $\gamma$ -ray energies to some extent (depending on pitch angle), and the atmospheric cascade would then be generated by a bunch of  $\gamma$ -rays of lower energy. Aharonian et al. [31] have considered this possibility and conclude that this bunch would appear as one air shower made up of the superposition of many sub-showers of lower energy where the LPM effect is negligible, the air shower having the energy of the initial  $\gamma$ -ray outside the geomagnetic field. If this is the case, then  $\gamma$ -rays above  $3 \times 10^{11}$  GeV would be observable by Fly's Eye, etc., and the upper limits presented in Figure 3 would stand, ruling out a TD origin for the  $2-3 \times 10^{11}$  GeV events. There is however, some uncertainty as to whether pair production will take place in the geomagnetic field. This depends on whether the geomagnetic field spatial dimension is larger than the formation length of the electron pair, i.e. the length required to achieve a separation between the two electrons which is greater than the classical radius of the electron. This question of whether or not pair production in the geomagnetic field takes place needs further investigation, but in any case TD models for the  $2-3 \times 10^{11}$  GeV events are either ruled out or severely constrained by our results.

---

[1] Hayashida N. *et al.* *Phys. Rev. Lett.* **73** 3491 (1994).

[2] Bird D.J. *et al.* *Ap. J.* **441** 144 (1995).

- [7] Aharonian, F.A., Bhattacharjee, P., and Schramm, D., *Phys. Rev. D* **46** 4188 (1992)
- [8] Bhattacharjee, P., Hill, C.T., and Schramm, D.N., *Phys. Rev. Lett.* **69** 567 (1992).
- [9] Gill, A.J., and Kibble, T.W.B., *Phys. Rev. D* **50** 3660 (1994).
- [10] Protheroe, R.J., and Johnson, P.A., *Astroparticle Phys.* **4** 253 (1996) and erratum (in press).
- [11] Sigl, G., Lee, S., Schramm, D.N., and Bhattacharjee, P., *Science* **270** 1977 (1995).
- [12] Sigl G. to appear in *Space Sci. Rev.* (1995)
- [13] Lee, S., *Phys. Rev D* submitted (1996).
- [14] Karle, A., *Phys. Lett. B*, **347** 161 (1995).
- [15] Protheroe, R.J., and Johnson, P.A., "Phenomenological Aspects of Underground Physics (TAUP95)", ed. M. Fratas, *Nucl. Phys. B., Proc. Suppl.*, **48**, (1996).
- [16] Sigl, G., Lee, S., and Coppi, P., *Phys. Rev. Lett* submitted (1996).
- [17] Clark, T.A., Brown, L.W., and Alexander, J.K., *Nature* **228**, 847 (1970)
- [18] Berezinsky V.S., *Yad. Fiz.* **11**, 339 (1970)
- [19] Protheroe, R.J., and Biermann, P.L., submitted (1996).
- [20] Protheroe, R.J., and Stanev, T., in preparation (1996)
- [21] Brandenburger, R., Pacific Conf. on Grav. and Cosmol. in press (World Scientific, Singapore, 1996)
- [22] Protheroe R.J. and Stanev T.S. *Mon. Not. R. Astron. Soc.* **264** 191 (1993).
- [23] Stecker F.W., De Jager O.C. and Salamon M.H. *Ap. J.* **390** L49 (1992).
- [24] Mather, J.C., et al., *Astrophys. J.* **420** 439 (1994)
- [25] Stanev T., in *Particle Acceleration in Cosmic Plasmas*, edited by G.P. Zank and T.K. Gaisser (AIP, New York, 1992) p.379.
- [26] Thompson, D.J., and Fichtel, C.E., *Astron. Astroph.* **109** 352 (1982).
- [27] Fichtel, C.E., *Proc. 3rd Compton Observatory Symposium, Astron. Astrophys. Suppl.* in press (1995).
- [28] Landau, L.D., and Pomeranchuk, I., *Dok. Akad. Nauk. SSSR* **92** 535 (1953); Migdal, A.B., *Phys. Rev.* **103** 1811 (1956).
- [29] Stanev, T., et al., *Phys. Rev. D* **25** 1291 (1982).
- [30] Erber, T., *Phys. Rev.* **38**, 626 (1968)
- [31] Aharonian, F.A., Kanevsky, B.L., and Sahakian, J., *J. Phys. G*, **17** 1909 (1991).

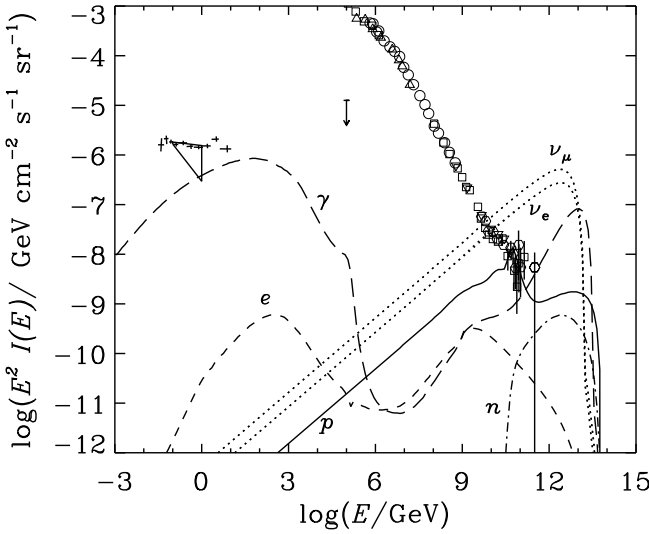


FIG. 1. Spectra at Earth for the topological defect model discussed in the text. SAS-2 and EGRET  $\gamma$ -ray data are shown at GeV energies, and HEGRA data at 100 TeV.

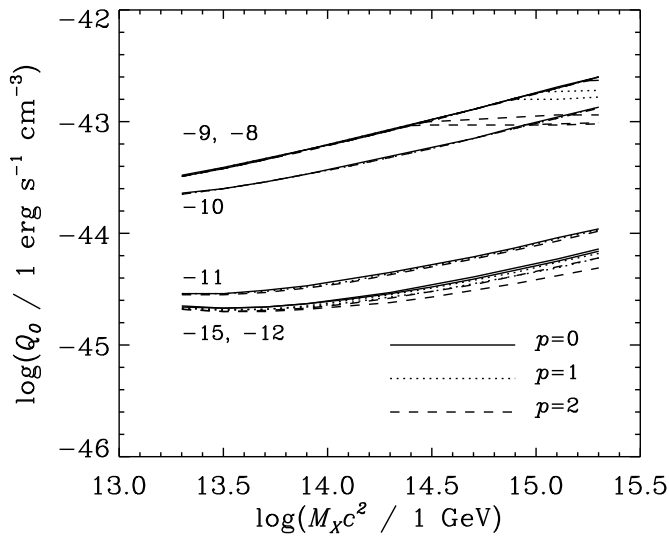


FIG. 2. Maximum rate of injection of energy in X-particles as a function of  $M_X$  for various magnetic fields and evolution models based on normalization of predicted intensity of “observable particles” to the  $3 \times 10^{11}$  GeV point, or using the  $\gamma$ -ray data as upper limits (the lower of the two is plotted). Numbers attached to curves give  $\log(B/1 \text{ G})$ .

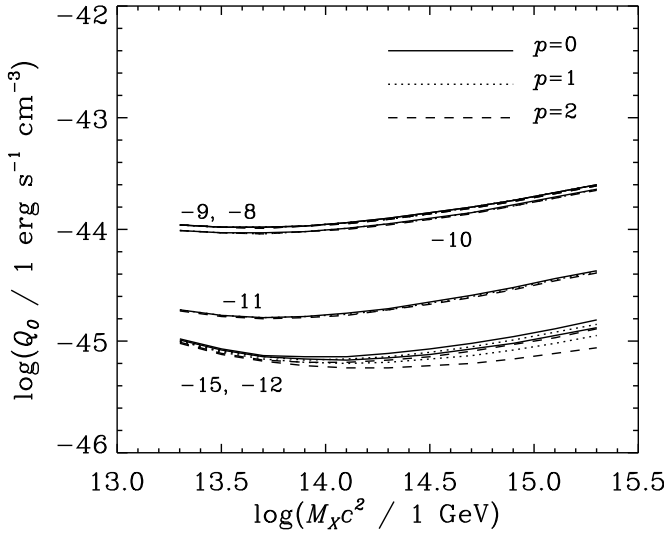


FIG. 3. Maximum rate of injection of energy in X-particles as a function of  $M_X$  for various magnetic fields and evolution models based on the non-observation of cosmic rays above  $3 \times 10^{11}$  GeV.

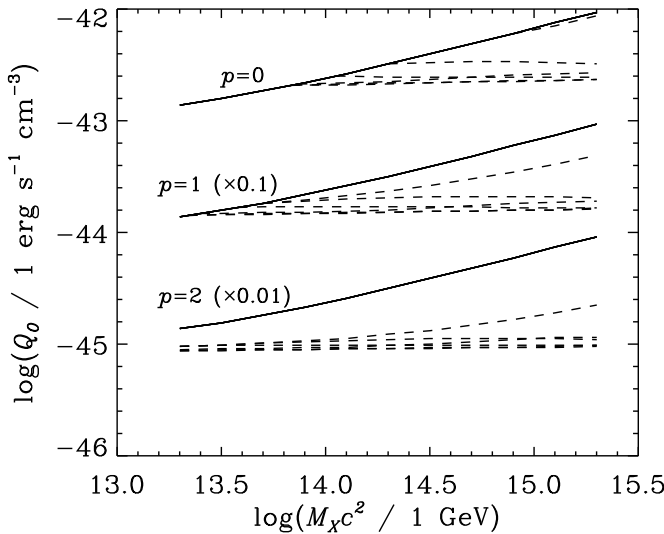


FIG. 4. Maximum rate of injection of energy in X-particles as a function of  $M_X$  for various magnetic fields and evolution models based on normalization of predicted intensity of nucleons (solid curves), and using the  $\gamma$ -ray data as upper limits (dashed curves) for  $B = 10^{-15}$  G (highest curves) to  $B = 10^{-8}$  G (lowest curves).